Magnetic force-based multiplexed immunoassay using superparamagnetic nanoparticles in microfluidic channel†

Kyu Sung Kim and Je-Kyun Park*

Received 15th February 2005, Accepted 11th April 2005
First published as an Advance Article on the web 29th April 2005
DOI: 10.1039/b502225h

This paper describes a novel microfluidic immunoassay utilizing binding of superparamagnetic nanoparticles to beads and deflection of these beads in a magnetic field as the signal for measuring the presence of analyte. The superparamagnetic 50 nm nanoparticles and fluorescent 1 μm polystyrene beads are immobilized with specific antibodies. When target analytes react with the polystyrene beads and superparamagnetic nanoparticles simultaneously, the superparamagnetic nanoparticles can be attached onto the microbeads by the antigen–antibody complex. In the poly(dimethylsiloxane) (PDMS) microfluidic channel, only the microbeads conjugated with superparamagnetic nanoparticles by analytes consequently move to the high gradient magnetic fields under the specific applied magnetic field. In this study, the magnetic force-based microfluidic immunoassay is successfully applied to detect the rabbit IgG and mouse IgG as model analytes. The lowest concentration of rabbit IgG and mouse IgG measured over the background is 244 pg mL^{-1} and 15.6 ng mL^{-1}, respectively. The velocities of microbeads conjugated with superparamagnetic nanoparticles are demonstrated by magnetic field gradients in microfluidic channels and compared with the calculated magnetic field gradients. Moreover, dual analyte detection in a single reaction is also performed by the fluorescent encoded microbeads in the microfluidic device. Detection range and lower detection limit can be controlled by the microbeads concentration and the higher magnetic field gradient.

Introduction

The development of robust, sensitive and high-throughput biosensors is one of the major issues in the area of nanobiotechnology.[1–5] Until now, some technical achievements for biological detection have been reported such as a diffusion-based immunoassay[6] and nanoparticle-based protein assays.[1–3,7] The use of nanoparticles in biological detection enhances the signal sensitivity of the sensor due to the various electronic and optical properties as a consequence of their dimensions.[3] Magnetic nanoparticles are also employed in biological detection and separation systems. Especially, superparamagnetic nanoparticles have single domain magnetic dipoles in an applied magnetic filed. Without an external magnetic field, they do not have permanent magnetic dipoles because the magnetic dipole–dipole interaction energy is weaker than thermal energy. Magnetic nanoparticles have biocompatibility, stability and an easily modifiable surface with biomolecules.[8] Moreover, magnetic nanoparticles could be manipulated on a microsystem.[9,10]

Recently, there have been many efforts to transform conventional biological works into a lab-on-a-chip by combining microfluidics with nanotechnology. This is because microfluidics helps to minimize the time and cost associated with routine biological analysis while improving reproducibility.[11] Some microbead-based analytical applications in microfluidic systems have been reported. They include microfluidic matrix coated beads,[12] magnetic beads,[13,14] packed bead beds[15] and bead suspensions.[16] Since the microbead has large surface area per unit volume, it can provide relatively large binding sites for biochemical reactions. Moreover, microbead-based assays have several advantages over the flat microarray, such as no washing steps, multiplexed assay using an encoded microbead, amplified signal due to large surface-to-volume ratio and short assay time because of the freely moveable microbeads in mediums.[16,17] Bead-based analysis is generally carried out using optical measurements in conjunction with flow cytometry.[18,19]

In this paper we have developed a novel biomolecular detection principle based on magnetic force in a microfluidic channel. It has been reported that magnetic beads were used to detect immunological reactions[20,21] and DNA hybridization,[22] and to separate blood cells.[18] In conventional immunoassay and separation with magnetic beads, a magnetic field was used to capture all of the magnetic beads and the fluorescent signal was employed to estimate the amount of antigen present in the sample. However, a magnetic field in this study was used to detect the biomolecules in a microfluidic channel. Although an ultrasensitive magnetic biosensor using a superconducting quantum interference device (SQUID) was developed for immunoassay, the disadvantage of this method is the limited analysis of single analyte based on the discrimination between bound and unbound magnetic nanoparticles.[23,24] This prevents the assay technique from wide biological application where multiple analytes should be detected in the same sample

† Electronic supplementary information (ESI) available: Determination of magnetic fields outside a rectangular magnet. See http://www.rsc.org/suppdata/lc/b5/b502225h/

*jekyun@kaist.ac.kr

solution. The proposed detection scheme is based on the fact that the specific polymer microbeads conjugated with superparamagnetic nanoparticles can only switch their path in microchannels when magnetic field induces magnetization of the attached superparamagnetic nanoparticles. This assay format is especially useful to construct a multiplexed assay platform in a microfluidic device or in a lab-on-a-chip. As shown in Fig. 1, the buffer and sample solution is injected into each side of the inlets. The sample solution contains the microbeads and magnetic nanoparticle complex. When antigen molecules (target analytes) simultaneously react with the microbeads and superparamagnetic nanoparticles which are immobilized by a specific antibody, the superparamagnetic nanoparticles will be attached onto the microbeads by the antigen–antibody complex. As a result, in a microfluidic channel, only the microbeads conjugated with superparamagnetic nanoparticles consequently move to the high gradient magnetic fields under the specific applied magnetic field. The flow in a microfluidic channel generally remains laminar, and the diffusion effects of the micro-sized beads are negligible. Therefore, the microbeads conjugated with superparamagnetic nanoparticles can change their flow path in an applied magnetic field. If the concentration of superparamagnetic nanoparticles on a microbead increases, the velocity of a microbead will increase because the velocity of microbeads is proportional to the total volume of the magnetic nanoparticles on a microbead and magnetic field gradient.[25] This implies that the target analytes in microfluidic channels are quantified by conjugated nanoparticles as a label or a magnetic force. In addition, since the microbeads have a fluorescent property, the path-changed microbeads can be identified by their own optical properties of fluorescent microbeads which can be encoded.[26] A detailed configuration of the microfluidic device is introduced, and assay design and its application as a multiplexed microfluidic immunoassay will also be discussed.

Theory

In a microchannel in which either width or height is less than 200 μm, an aqueous flow is generally laminar, not turbulent. At the perpendicular direction against the flow direction there is no force on the microbead. However, when the microbeads are conjugated with the superparamagnetic nanoparticles under the applied magnetic field, they will move against the flow direction due to the magnetic force on each labeled superparamagnetic nanoparticle on the microbead. The magnetic force, $\boldsymbol{F}_{sm}$, on a superparamagnetic nanoparticle in the aqueous solution is given by eqn. (1):[25]

$$\boldsymbol{F}_{sm} = \frac{1}{2}\frac{V_{sm}\Delta\chi_{sm}}{\mu_0}\nabla\boldsymbol{B}^2 \quad (1)$$

where V_{sm} is the volume of the superparamagnetic nanoparticle, $\Delta\chi_{sm}$ is the net magnetic susceptibility of a superparamagnetic nanoparticle in aqueous solution, $\boldsymbol{B}$ is the magnetic field and μ_0 is the vacuum permeability. This equation is originally derived from $\boldsymbol{F}_{sm} = (\boldsymbol{m}\nabla)\boldsymbol{B}$, where $\boldsymbol{m}$ is magnetic dipole. The total moment on a particle can be written $\boldsymbol{m} = V_{sm}\boldsymbol{M}$. The magnetization of a superparamagnetic nanoparticle can be converted to $\boldsymbol{M} = \Delta\chi_{sm}\boldsymbol{H}$, where $\boldsymbol{H}$ is external magnetic field. Using $\boldsymbol{B} = \mu_0\boldsymbol{H}$, eqn. (1) is obtained. This equation is valid for magnetic fields which do not saturate the magnetization value of a superparamagnetic nanoparticle. If external magnetic fields are enough to saturate the magnetization of a superparamagnetic nanoparticle, magnetic force is not proportional to $\nabla\boldsymbol{B}^2$ but proportional to $\nabla\boldsymbol{B}$. When the superparamagnetic nanoparticles are conjugated with the microbeads, the applied magnetic field will induce the magnetic force on superparamagnetic nanoparticles. Then the total magnetic force of the superparamagnetic nanoparticles on the microbeads will cause microbeads to move. The total magnetic force, $\boldsymbol{F}_{tsm}$, of the superparamagnetic nanoparticles on the microbead is the sum of the magnetic forces acting on each superparamagnetic nanoparticle on the microbead:

$$\boldsymbol{F}_{tsm} = N_{sm}\boldsymbol{F}_{sm} = \frac{1}{2}N_{sm}\frac{V_{sm}\Delta\chi_{sm}}{\mu_0}\nabla\boldsymbol{B}^2 \quad (2)$$

where N_{sm} is the number of the superparamagnetic nanoparticle conjugated with a microbead. If the superparamagnetic nanoparticles are a specific size, the volume (V_{sm}) and the magnetic susceptibility (χ_{sm}) of each superparamagnetic nanoparticle have the same value because V_{sm} and χ_{sm} are the variables of particle size. Therefore in the specific magnetic field gradient ($\nabla\boldsymbol{B}^2$), the $\boldsymbol{F}_{tsm}$ is determined by the number of the superparamagnetic nanoparticle.

When the microbeads are moved by the total magnetic force, the Stokes' drag force ($\boldsymbol{F}_D$) is generated against the apposite direction of the moving microbeads. The $\boldsymbol{F}_D$ is represented by the following eqn. (3):

$$\boldsymbol{F}_D = -6\pi R_M\eta\boldsymbol{v} \quad (3)$$

where R_M is the radius of the microbead, η is the viscosity of the aqueous medium and $\boldsymbol{v}$ is the velocity of the microbead. The $\boldsymbol{v}$ of the microbead results from the magnetic force. Since the direction of the magnetic force is the perpendicular direction of fluid flow and the microbeads move in the laminar flow, the $\boldsymbol{F}_D$ equals the $-\boldsymbol{F}_{tsm}$.

$$\boldsymbol{F}_D = -\boldsymbol{F}_{tsm} \quad (4)$$

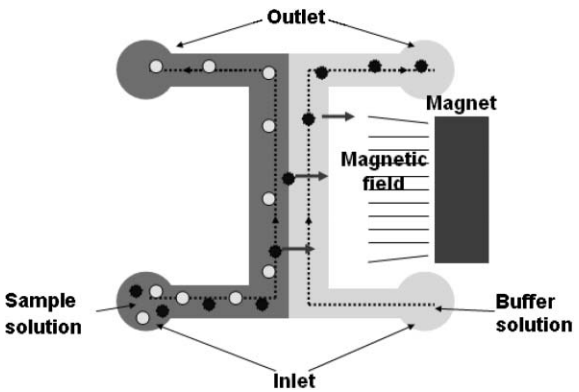

Fig. 1 Proposed detection principle. Microbead conjugated with superparamagnetic nanoparticles (●). Unconjugated microbead (○).

Combining eqn. (2) and eqn. (3) into eqn. (4), the velocity of the microbeads in the aqueous medium is represented by the following eqn. (5):

$$v = \frac{N_{sm} V_{sm} \Delta\chi_{sm}}{12\pi R_M \eta\mu_0} \nabla \boldsymbol{B}^2 \quad (5)$$

Therefore, when the size of the superparamagnetic nanoparticle and the microbead is assumed to be uniform respectively, the velocity of the microbead is decided by the number of the superparamagnetic nanoparticle conjugated on the microbead (N_{sm}) and the magnetic field gradient.

Experimental

Design and fabrication of the microfluidic device

Fig. 2(a) shows the configuration of the microfluidic device. The microfluidic device had two inlets and one outlet. One of the inlets, the right one, is for the reacted sample solutions, and another inlet, the left one, is for the buffer solutions. A junction part of two inlets is for hydrodynamic focusing (Fig. 2(b)). The hydrodynamically focused sample solutions will flow through a 10 mm long microchannel which leans toward one side of the device. The leaned microchannel will have an influence on the high magnetic field gradients. At the branches of microchannels before the outlet, molecular detection would be recognized by flow paths of microbeads as shown in Fig. 2(c). The hydrodynamically focused microbeads of sample solution will flow through the 105 μm width channel of the outlet. However, when the microbeads are conjugated with the superparamagnetic nanoparticles, they will switch their flow path and flow through the 95 μm wide channel of the outlet under the applied magnetic fields.

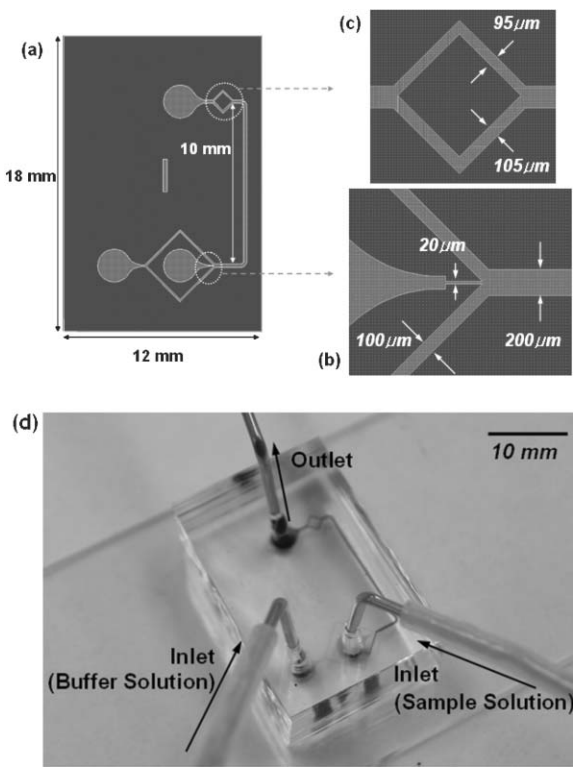

Fig. 2 (a) Layout of the device which has two inlets and one outlet. (b) At the part of the inlet, sample solution was hydrodynamically focused. (c) The focused sample solution flowed through the 105 μm wide channel before the outlet. (d) A photograph of the fabricated device.

The microfluidic device was fabricated by a conventional poly(dimethylsiloxane) (PDMS) (Sylgard 184, Dow Corning) molding processes. The positive photoresistor (AZ9260) was coated on the bare Si wafer to create molds. The coating speed was set at 6000 rpm for 60 s to make the 5.5 μm thickness which was the height of the microchannel. The photoresistor was patterned using UV lithography. After the patterning, the prepared mixture of PDMS was degassed under vacuum, poured onto the mold and cured for 30 min at 100 °C on the hot plate. The cured PDMS was peeled from the mold and rinsed in the ethanol. The slide glass was rinsed in the heptane. Inlet and outlet holes were punched before the PDMS rinsing step. The rinsed PDMS and slide glass were dried in the dry oven at 80 °C and treated by air plasma (200 mTorr, 200 W) using an expanded plasma cleaner (Harrick Science, Ossing, NY) for 20 s. Then, the PDMS and slide glass were bonded immediately. Fig. 2(d) shows a photograph of the fabricated device.

Materials

Bovine serum albumin (BSA) was obtained from Sigma Chemical Company (St. Louis, MO). Tween® 20 was obtained from Aldrich (St. Louis, MO). One liter phosphate buffered saline (PBS) contained 8 g of NaCl, 0.2 g of KCl, 1.44 g of Na_2HPO_4 and 0.24 g of KH_2PO_4. The pH was adjusted to 7.4 with HCl. All solutions were prepared using deionized water with Millipore (Milli-Q, Millipore Co., MA) and autoclaved water. All chemicals used were of analytical reagent grade. The red fluorescent microbeads (excitation 580/emission 605) immobilized with NeutrAvidin molecules were purchased from Molecular Probes (Eugene, OR). The microbeads (1 μm diameter) were brought into solution in 0.4 mL of aqueous suspensions containing 1% solids, 50 mM sodium phosphate, 50 mM NaCl, pH 7.5, 0.02% Tween® 20 and 5 mM azide. The concentration of the red fluorescent microbeads was 1.4×10^{10} beads mL^{-1}. The binding capacity of the NeutrAvidin molecules of the fluorescent microbeads was 4.8 nmol mg^{-1}. The YG fluorescent microbeads (excitation 441/emission 486) immobilized with goat anti-mouse IgG (H&L) were bought from Polysciences, Inc. (Warrington, PA). The microbeads (1 μm diameter) were brought into solution in 1 mL of as aqueous suspensions containing 1.23% solids, 20 mM sodium phosphate, 8 mg mL^{-1} NaCl, pH 7.4, 1% BSA, 0.1% sodium azide and 5% glycerol. The concentration of the microbeads was 2.18×10^{10} beads mL^{-1}. The protein concentration in the microbead solution is approximately 268 μg mL^{-1}. Two kinds of superparamagnetic nanoparticle solution were obtained from Miltenyi Biotec (Bergisch Gladbach, Germany). The superparamagnetic nanoparticles in each solution were conjugated to goat polyclonal anti-mouse IgG (H+L) $F(ab')_2$ fragments and goat polyclonal anti-rabbit IgG (H+L) $F(ab')_2$ fragments, respectively. The superparamagnetic nanoparticles consist of iron oxide and their size was about 50 nm diameter

including polymer coating and proteins on surface. The superparamagnetic nanoparticles conjugated to goat anti-mouse IgG (H+L) $F(ab')_2$ fragments and goat anti-rabbit IgG (H+L) $F(ab')_2$ fragments were supplied as 0.5 mL solution containing 0.1% BSA and 0.05% sodium azide. Normal rabbit IgG, mouse IgG, goat anti-rabbit IgG biotin conjugates were purchased from Santa Cruz Biotechnology Inc. (Santa Cruz, CA).

Preparation of microbeads

The solutions of the YG fluorescent microbeads immobilized with goat anti-mouse IgG and the red fluorescent microbeads immobilized with NeutrAvidin molecules were prepared for sandwich immunoassay. The solution of the YG fluorescent microbeads was washed two times using a centrifuge at 13,000 g for 5 min in pH 7.4 PBS containing 0.1% BSA and 0.02% Tween® 20 and diluted into pH 7.4 PBS containing 0.1% BSA before immunoassay. For preparation of anti-rabbit IgG conjugated microbeads, the red fluorescent microbeads immobilized with NeutrAvidin molecules and goat anti-rabbit IgG biotin conjugate were used. The solution of the red fluorescent microbeads was diluted by 1.4×10^7 beads $(100\ \mu L)^{-1}$ in pH 7.4 PBS and 1% BSA. Then, 100 μL of the biotin conjugated goat anti-rabbit IgG solution which was diluted in PBS and 1% BSA to a concentration of 250 nM was added. After the mixture was incubated for 30 min at room temperature with gentle mixing, the reacted microbeads were pelleted by a centrifuge at 13,000 g for 5 min. Then, the supernatant was removed and the pelleted microbeads were resuspended by vortex and sonication for 15 s in pH 7.4 PBS containing 0.1% BSA and 0.02% Tween® 20 in order to remove the unbound anti-rabbit IgG biotin. These washing steps were repeated three times. The prepared microbead solutions were stored at 4 °C in the dark before use. The concentration of microbeads was measured by counting the beads in a defined volume. The microbeads were counted by a hemacytometer (Marienfeld, Germany).

Measurement setup

The microfluidic device was placed on an inverted microscope (Zeiss Axiovert 25, Carl Zeiss, Germany) with a 50 W mercury lamp of light source for excitation of fluorescent microbeads (Fig. 3). A CCD camera (Nikon, Japan) was integrated on the inverted microscope to capture images of the movement of fluorescent microbeads. The microfluidic device had two inlets, one outlet and an extraction part. The tubing was inserted into the holes of the device to connect the 10 μL and 100 μL microsyringes (1700 series gastight syringes, Hamilton Company, NV). The microsyringes were connected with another side of tubing to pump the aqueous medium by a dual syringe pump (Pump 11 Pico Plus, Harvard Apparatus, Inc., MA). The reacted sample solutions were injected through one of the inlets and the buffer solution (PBS, 0.1% BSA, pH 7.4) was injected through another inlet. In order to apply magnetic fields, we used NdFe35 permanent magnet (Magtopia, Korea) which was $50 \times 25 \times 10\ mm^3$ and Br = 12,000 gauss. The permanent magnet was placed at one side of the microchannel and manually moved using a linear moving stage (M-460A-XYZ, Newport Corporation, CA). The movement of fluorescent microbeads conjugated with the superparamagnetic nanoparticles occurred at the hydrodynamic focused region of the microchannel in the applied magnetic fields. After the sample and buffer solutions were loaded and pumped using a dual syringe pump, the images of movement of fluorescent microbeads of one sample solution were captured with 5 min and the velocities were analyzed manually. The images of the movement of fluorescent microbeads were captured by avi format using a CCD camera. Then, avi images were divided into many frames of still images to measure the distance of the movement of fluorescent microbeads. The specific coordinates of the fluorescent microbeads were found by the Photoshop (Adobe Systems Inc.). Then, the velocities of fluorescent microbeads could be determined. Each data point of the velocity measurements represented the mean value of at least three microbeads data.

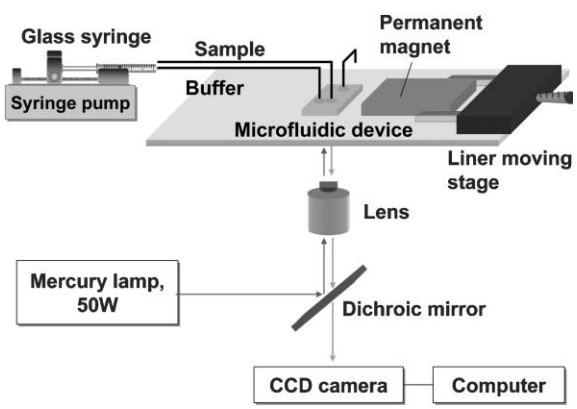

Fig. 3 Experimental setup of the microfluidic device.

Microfluidic sandwich immunoassay procedure

The sandwich immunoassay used in this study had no washing step and all-in-one reaction type. All reactions were also performed in 1.5 mL microcentrifuge tubes. The selected concentrations of the fluorescent microbeads conjugated with antibodies were aliquoted by 70 μL in a microcentrifuge tube. After the 2-fold serial dilutions of antigen (mouse IgG, rabbit IgG) in pH 7.4 PBS containing 0.1% BSA, 10 μL of antigen sample solution was added to each aliquot 70 μL of the microbead solution in microcentrifuge tubes. In order to observe backgrounds, each experiment included a nonspecific binding control in which 10 μL of pH 7.4 PBS containing 0.1% BSA was added. The mixture solution was mixed and incubated for 10 min at room temperature. Then, 5 μL of the solution of the antibody immobilized superparamagnetic nanoparticles as the labels of sandwich immunoassay was added to each mixture solution. Here, the volume and concentration of the solution of superparamagnetic nanoparticles were fixed. The mixture solution was mixed and incubated for another 20 min at room temperature, followed by injection of these sample solution into the microchannel using syringe pump to measure the velocity of microbeads. The flow rates in the y-direction (flow direction) were not fixed but were almost zero to observe the movement of microbead in the x-direction of the magnetic field gradient easily. The velocities were

measured only in the x-direction. The permanent magnet was fixed at 2 mm apart from the microbeads except for experiments with magnetic field variation.

Variation of magnetic fields

A NdFe35 permanent magnet was used for variation effect of magnetic fields. The concentration of the red fluorescent microbeads conjugated with anti-rabbit IgG was 2.55×10^5 beads $(70\ \mu L)^{-1}$. A volume of antigen solution was 10 μL of rabbit IgG with 1 μg mL^{-1}. The solution of the superparamagnetic nanoparticles conjugated to anti-rabbit IgG was 5 μL. The permanent magnet was placed at the side of the microfluidic device. In this experiment, the microchannel was aligned from $y = 7.5$ mm to $y = 12.5$ mm at $x = 1, 2, 3, 4, 5, 6, 7$ mm and $z = 1$ mm. The velocities were measured only in the x-direction.

Dual analyte detection

The concentration of the red fluorescent microbeads conjugated with anti-rabbit IgG was 1.77×10^6 beads $(70\ \mu L)^{-1}$. The concentration of the green-yellow fluorescent microbeads conjugated with anti-mouse IgG was 2.12×10^6 beads $(70\ \mu L)^{-1}$. The solutions of red and green-yellow fluorescent microbeads were mixed in the same microcentrifuge tube. Then, 10 μL of rabbit IgG with 250 ng mL^{-1} and 10 μL of mouse IgG with 125 ng mL^{-1} were added at the same time. The mixture was mixed and incubated for 10 min at room temperature. Then, 5 μL solution of the superparamagnetic nanoparticles conjugated to anti-rabbit IgG and 5 μL solution of the superparamagnetic nanoparticles conjugated to anti-mouse IgG were also added at the same time. The mixture solution was mixed and incubated for another 20 min at room temperature. The flow rates of buffer solution and reacted sample solution were 120 nL min^{-1} by 100 μL glass syringe and 12 nL min^{-1} by 10 μL glass syringe using dual syringe pump, respectively. The shifts of flow path were observed at the branches of microchannels before the outlet, Fig. 2(c).

Results and discussion

Microfluidic sandwich immunoassay

Sandwich immunoassay was performed using the YG fluorescent microbeads immobilized with goat anti-mouse IgG and the red fluorescent microbeads immobilized with goat anti-rabbit IgG. The red fluorescent microbeads conjugated to goat anti-rabbit IgG *via* avidin bridges were used in this experiment for detection of rabbit IgG. The concentration of the red fluorescent microbeads was 2.55×10^5 beads $(70\ \mu L)^{-1}$ in a 1.5 mL microcentrifuge tube. The volume of antigen solution was 10 μL of rabbit IgG with different concentrations. A control experiment was carried out with 10 μL of 0.1% BSA in PBS instead of rabbit IgG. As shown in Fig. 4(a), a background velocity was not observed without only the oscillation due to the diffusion effect. The background velocity was below 0.05 μm s^{-1}. This image showed that the laminar flow stream was in the direction of the positive y-axis and the magnetic field gradient was in the x-axis direction. On the other hand, the mean value of velocity at the 250 ng mL^{-1} of rabbit IgG was 2.39 ± 0.3 μm s^{-1} (Fig. 4(b)).

As shown in Fig. 5(a), the velocities of the microbeads were measured over a range of concentration of rabbit IgG from 1 ng mL^{-1} (6.25 pM) to 1 μg mL^{-1} (6.25 nM). The lowest concentration of rabbit IgG that was measured over the background was almost 244 pg mL^{-1}(1.5 pM). The velocity was almost saturated at about 1 μg mL^{-1}. The reason for the saturated velocity can be explained by the limited binding capacity of the microbead surface.

We carried out an additional assay of rabbit IgG under the same conditions but a different concentration of microbeads. The concentration of microbeads was sevenfold, 1.77×10^6 beads $(70\ \mu L)^{-1}$. As shown in Fig. 5(a), the range of detectable concentration was shifted to the right compared with the above experiment of the different concentrations of microbeads, 2.55×10^5 beads $(70\ \mu L)^{-1}$. This is because of the total surface area of the microbeads which is the factor of the range of molecular detectable concentrations. From the result it seems that the detection ranges can be adjusted by changing the concentration of the microbeads. The variation was between 8.0 to 12.8% CV for 2.55×10^5 beads $(70\ \mu L)^{-1}$, while between 5.4 to 18.8% CV for 1.77×10^6 beads $(70\ \mu L)^{-1}$ at a given analyte concentration. In the case of measurement of rabit IgG concentration based on the 2.55×10^5 beads $(70\ \mu L)^{-1}$, the precision of the velocity measurement showed errors of less than 11.6% analyte concentration.

The YG fluorescent microbeads conjugated to goat anti-mouse IgG were also carried out in this sandwich immunoassay. The concentration of the YG fluorescent microbeads

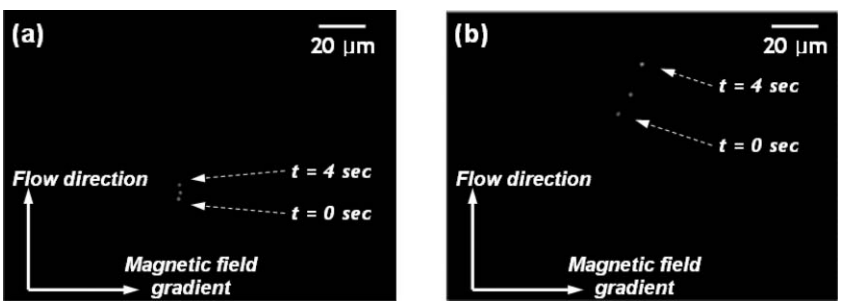

Fig. 4 CCD images of migrations of reacted fluorescent microbead by magnetic fields in the channel 2 mm apart from the magnet. Interval time: 2 s. (a) The analyte was 10 μL PBS (0.1% BSA, pH 7.4) for the background. The velocity of the control experiment was below 0.05 μm s^{-1}. (b) The analyte was 10 μL of 250 ng mL^{-1} rabbit IgG. The velocity was 2.39 ± 0.3 μm s^{-1}.

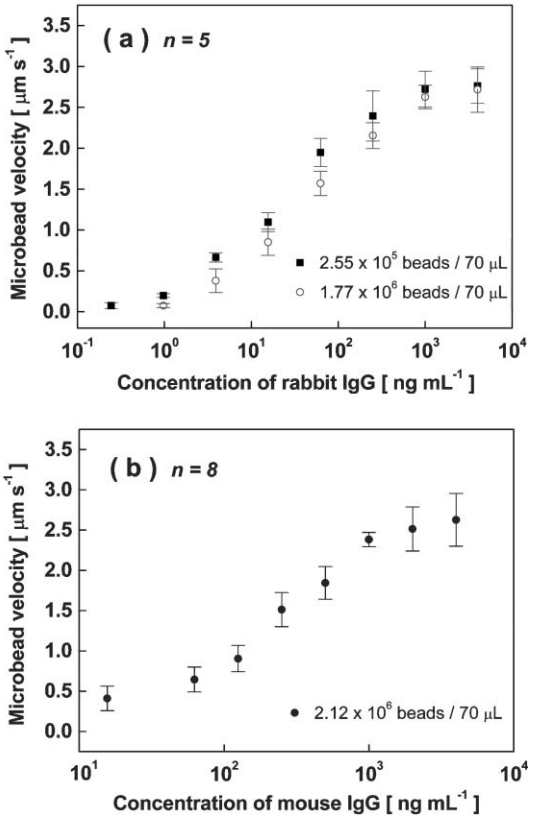

Fig. 5 (a) Results of magnetic force-based microfluidic sandwich immunoassay for detection of rabbit IgG. Rabbit IgG detection was feasible over a concentration range 1 ng mL^{-1} to 1 μg mL^{-1}. (b) The dynamic range of mouse IgG was 62.5 ng mL^{-1} to 2 μg mL^{-1}.

was 2.12×10^6 beads $(70\ \mu L)^{-1}$. The volume of antigen solution was 10 μL of mouse IgG with different concentrations. As shown in Fig. 5(b), the velocities of the microbeads were measured over a range of concentration of mouse IgG from 62.5 ng mL^{-1} to 2 μg mL^{-1}. The variation was between 3.7 to 18.0% CV for 2.12×10^6 beads $(70\ \mu L)^{-1}$ at a given analyte concentration. The lowest concentration of mouse IgG that was measured over the background was almost 15.6 ng mL^{-1}. The velocity was almost saturated at about 2 μg mL^{-1}.

Effect of the magnetic fields variation

Movements of microbeads conjugated with magnetic nanoparticles are affected by gradients of magnetic fields. To evaluate the magnetic fields and magnetic field gradients, the magnetic fields outside a rectangular magnet were calculated using MATLAB (The MathWorks, MA) (see ESI†). The calculation results show that the velocities of microbeads conjugated with magnetic nanoparticles are proportional to the magnetic field gradient, $\nabla \boldsymbol{B}$. In addition, the magnetic field gradient along the y-axis, $d\boldsymbol{B}_y/dy$, is much less than the magnetic field gradient along the x-axis, $d\boldsymbol{B}_x/dx$. Therefore, the effect of the magnetic field gradient along the y-axis, $d\boldsymbol{B}_y/dy$, could be nearly ignored.

The experimental results were also obtained at the same locations as the calculated condition. As shown in Fig. 6,

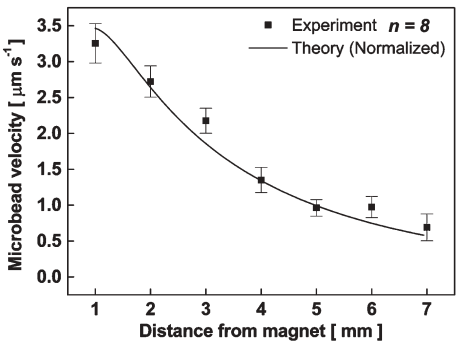

Fig. 6 Experimental results of the reacted microbeads with different magnetic field gradients (closed square). The magnet was moved to the side of the microchannel from 1 mm to 7 mm when the concentration of rabbit IgG was 1 μg ml^{-1}. The theoretical values of magnetic field gradient along the x-axis, $d\boldsymbol{B}_x/dx$, was normalized and folded over the same graph.

the velocities were inversely proportional to the distance from the magnet as the magnetic field gradient along the x-axis is decreased. In order to compare experiment with theory, the magnetic field gradient along the x-axis, $d\boldsymbol{B}_x/dx$ was normalized and folded over the same graph (Fig. 6). The normalized values were well correlated with the experimental values. Therefore, the velocity of the reacted microbeads could be manipulated by changing the magnetic field gradients.

In this experimental setup, the magnetic field gradient was below 0.35 T mm^{-1}. Recently, there were some attempts to manipulate magnetic particles on a micro electromagnet chip.[9,10,27,28] These studies showed that maximum values of magnetic field gradients were from 0.1 T mm^{-1} to several hundreds of T mm^{-1} on their own micro electromagnet chip.[10,27,29,30] In addition, a high magnetic field gradient, 10^3–10^4 T mm^{-1}, was generated using metallic rods by specific design.[31] Specific design of material on a chip can be applied in order to generate a high magnetic field gradient. Therefore, a micro electromagnet instead of a permanent magnet will be promised for higher sensitivity and lower detection limit.

Dual analyte detection

Dual analyte detection was also performed by an all-in-one reaction. The flow rates of buffer solution and the reacted sample solution were 120 nL min^{-1} by 100 μL glass syringe and 12 nL min^{-1} by 10 μL glass syringe using dual syringe pump, respectively. The velocity of the hydrodynamically focused microbeads was about 3.3 mm s^{-1}. The reacted microbeads in no magnetic field gradient were flowed along their own focused line, Fig. 7(a). The microbeads flowed along their own focused line and maintained their flow path. However, when the magnet was 4 mm apart from the microbeads, the flow path of red fluorescent microbeads was shifted and then the red fluorescent microbeads flowed through the upward channel, but green-yellow fluorescent microbeads were kept to their own flow path, Fig. 7(b). From Fig. 5 and 6, the velocity of microbeads by the magnetic field gradient could be estimated. The estimated velocities of

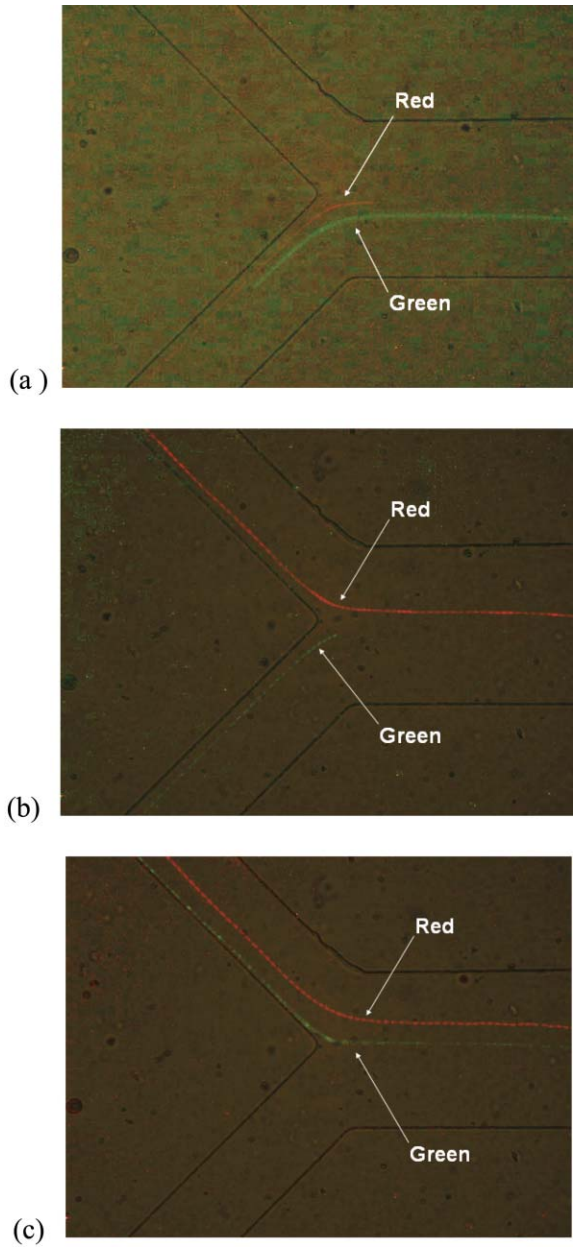

Fig. 7 CCD images of fluorescent microbeads. Original background images of fluorescent microbeads were dark, but a microchannel image on the same place was folded on the original images in order to show the trace of the microbeads. (a) The trace of the microbeads without a permanent magnet. The microbeads flowed along their own focused line and maintained their flow path. (b) The trace of the microbeads with a permanent magnet which was 4 mm apart from the microbeads. The flow path of only the red fluorescent microbeads was shifted by the magnetic field gradient. (c) The trace of the microbeads with a permanent magnet 2 mm apart from microbeads. The flow paths of both the red fluorescent microbeads and green-yellow fluorescent microbeads were switched to the upward channel by the magnetic field gradient.

red and green-yellow microbeads are about 1.30 μm s^{-1} and 0.48 μm s^{-1}, respectively. When the magnet was 2 mm apart from microbeads, the flow paths of both red and green-yellow fluorescent microbeads were switched to the upward channel, Fig. 7(c). As shown in Fig. 5, the velocities of red and green-yellow microbeads are 2.15 ± 0.16 μm s^{-1} and 0.90 ± 0.16 μm s^{-1}, respectively.

These results show that the magnetic force detection scheme could be utilized in multiplexed biological assays. In this paper, dual analyte detections were carried out by changing magnetic field gradients using two different types of microbeads at the same time. Using the same strategy, multiplexed assays are possible in a single reaction with these various encoded microbeads.[32] Recently, encoded microbeads using quantum dots were developed[26,33] and fluid-based DNA microarrays were studied.[34] Those microbeads were encoded by ratios of different colored quantum dots. Over 1000 ratios are distinguishable with three colors only.[33]

Conclusions

We have performed the magnetic force-based microfluidic immunoassay using microbeads and magnetic nanoparticles. The magnetic force-based immunoassay was devised first and successfully applied to detect the rabbit IgG and mouse IgG as the model analyte of microfluidic sandwich immunoassay. The movements of microbeads conjugated with magnetic nanoparticles were demonstrated by magnetic field gradients. Experimental results for the variation of magnetic field corresponded to the normalized values of calculated magnetic field gradient. High magnetic field gradients using micro electromagnets could be applied to this detection method for high sensitivity and lower detection limit. Dual analyte detection of rabbit IgG and mouse IgG in a single reaction was carried out in a microfluidic device. The multiplexed immunoassay using an encoded microbead which is immobilized with a certain antibody could be possible using this detection principle. The detections were made distinguishable by switching of the flow path of the microbeads from captured CCD images. However, adding experimental setups such as a photomultiplier tube and an automated moving stage for a magnet or an electromagnet, immunoassays could be automated and be more efficient. Already mentioned above, the manipulation of magnetic microbeads or nanoparticles in a microsystem has been studied by other groups. In those reports, the values of magnetic field gradients on micro electromagnetic chips were much higher over three orders than this permanent magnet system. With such micro electromagnetic integrated systems, a high performance, high sensitivity, and low detection limited assay system could be developed. Moreover, this detection scheme could be utilized in a lab-on-a-chip or in a μ-TAS device.

Acknowledgements

This work was supported by the CHUNG Moon Soul Center for BioInformation and BioElectronics, KAIST. The microfabrication work was performed at the Digital Nanolocomotion Center.

Kyu Sung Kim and Je-Kyun Park*
Department of BioSystems, Korea Advanced Institute of Science and Technology, 373-1 Guseong-dong, Yuseong-gu, Daejeon 305-701, Korea. E-mail: jekyun@kaist.ac.kr; Fax: 82 42 869 4310; Tel: 82 42 869 4315

References

1 C. M. Niemeyer, *Angew. Chem. Int. Ed. Engl.*, 2001, **40**, 4128–4158.★*This review was focused on the use of nanoparticles at the intersection of materials research, nanosciences, and molecular biotechnology*.
2 A. P. Alivisatos, *Nat. Biotechnol.*, 2004, **22**, 47–52.
3 A. N. Shipway, E. Katz and I. Willner, *ChemPhysChem*, 2000, **1**, 18–52.
4 T. G. Drummond, M. G. Hill and J. K. Barton, *Nat. Biotechnol.*, 2003, **21**, 1192–1199.
5 L. Mazzola, *Nat. Biotechnol.*, 2003, **21**, 1137–1143.★*This paper summarized the commercial efforts using nanotechnology in life sciences and research trends on nanobiotechnology*.
6 A. Hatch, A. E. Kamholz, K. R. Hawkins, M. S. Munson, E. A. Schilling, B. H. Weigl and P. Yager, *Nat. Biotechnol.*, 2001, **19**, 461–465.
7 J. M. Nam, C. S. Thaxton and C. A. Mirkin, *Science*, 2003, **301**, 1884–1886.
8 I. Šafařík and M. Safaříková, *Monatsh. Chem.*, 2002, **133**, 737–759.★*This review describes well information about magnetic nanoparticles and their applications in various areas of biosciences and biotechnologies*.
9 E. Mirowski, J. Moreland, S. E. Russke and M. J. Donahue, *Appl. Phys. Lett.*, 2004, **84**, 1786–1788.
10 C. S. Lee, H. Lee and R. M. Westervelt, *Appl. Phys. Lett.*, 2001, **79**, 3308–3310.
11 P. Mitchell, *Nat. Biotechnol.*, 2001, **19**, 717–721.
12 N. Malmstadt, P. Yager, A. S. Hoffman and P. S. Stayton, *Anal. Chem.*, 2003, **75**, 2943–2949.
13 Z. H. Fan, S. Mangru, R. Granzow, P. Heaney, W. Ho, Q. Dong and R. Kumar, *Anal. Chem.*, 1999, **71**, 4851–4859.
14 J. W. Choi, K. W. Oh, J. H. Thomas, W. R. Heineman, H. B. Halsall, J. H. Nevin, A. J. Helmicki, H. T. Henderson and C. H. Ahn, *Lab Chip*, 2002, **2**, 27–30.
15 A. B. Jemere, R. D. Oleschuk, F. Ouchen, F. Fajuyigbe and D. J. Harrison, *Electrophoresis*, 2002, **23**, 3537–3544.
16 J. P. Nolan and L. A. Sklar, *Trends Biotechnol.*, 2002, **20**, 9–12.
17 E. Verpoorte, *Lab Chip*, 2003, **3**, 60N–68N.★*A good overview of bead-based assays in microfluidic systems*.
18 H. Nishi, S. Nishimura, M. Higashiura, N. Ikeya, H. Ohta, T. Tsuji, M. Nishimura, S. Ohnishi and H. Higashi, *J. Immunol. Methods*, 2000, **240**, 39–46.
19 Z. Wang, J. El-Ali, M. Engelund, T. Gotsaed, I. R. Perch-Nielsen, K. B. Mogensen, D. Snakenborg, J. P. Kutter and A. Wolff, *Lab Chip*, 2004, **4**, 372–377.
20 X. Zhao and S. A. Shippy, *Anal. Chem.*, 2004, **76**, 1871–1876.
21 M. A. Hayes, N. A. Polson, A. N. Phayre and A. A. Garcia, *Anal. Chem.*, 2001, **73**, 5896–5902.
22 R. L. Edelstein, C. R. Tamanaha, P. E. Sheehan, M. M. Miller, D. R. Baselt, L. J. Whitman and R. J. Colton, *Biosens. Bioelectron.*, 2000, **14**, 805–813.
23 Y. R. Chemla, H. L. Grossman, Y. Poon, R. McDermott, R. Stevens, M. D. Alper and J. Clarke, *Proc. Natl. Acad. Sci. USA*, 2000, **97**, 14268–14272.
24 K. Enpuku, D. Kuroda, A. Ohba, T. Q. Yang, K. Yoshinaga, T. Nakahara, H. Kuma and N. Hamasaki, *Jpn. J. Appl. Phys.*, 2003, **42**, L1436–L1438.
25 M. Zborowski, C. B. Fuh, R. Green, L. Sun and J. J. Chalmers, *Anal. Chem.*, 1995, **67**, 3702–3712.
26 M. Han, X. Gao, J. Z. Su and S. Nie, *Nat. Biotechnol.*, 2001, **19**, 631–635.
27 T. Deng, M. Radhakrishnan, G. Zabow, M. Prentiss and G. M. Whitesides, *Appl. Phys. Lett.*, 2001, **78**, 1775–1777.
28 C. Chiou, Z. Tseng and G. Lee, *Proceedings of the IEEE 17th International Conference on Micro Electro Mechanical Systems (IEEE MEMS 2004)*, Maastricht, The Netherlands, January 25–29, 2004, pp. 613–616.
29 M. Drndic, K. S. Johnson, J. H. Thywissen, M. Prentiss and R. M. Westervelt, *Appl. Phys. Lett.*, 1998, **72**, 2906–2908.
30 N. H. Dekker, C. S. Lee, V. Lorent, J. H. Thywissen, S. P. Smith, M. Drndic, R. M. Westervelt and M. Prentiss, *Phys. Rev. Lett.*, 2000, **84**, 1124–1127.
31 A. R. Urbach, J. C. Love, M. G. Prentiss and G. M. Whitesides, *J. Am. Chem. Soc.*, 2003, **125**, 12704–12705.
32 T. O. Joos, D. Stoll and M. F. Templin, *Curr. Opin. Chem. Biol.*, 2001, **6**, 67–80.
33 X. Gao and S. Nie, *J. Phys. Chem. B*, 2003, **107**, 11575–11578.
34 K. E. Meissner, E. Herz, R. P. Kruzeclock and W. B. Spillman Jr., *Phys. Status Solidi C*, 2003, 1355–1359.